J. metamorphic Geol., 2002, **20,** 529–541

K-rich fluid metasomatism at high-pressure metamorphic conditions: Lawsonite decomposition in rodingitized ultramafite of the Maksyutovo Complex, Southern Urals (Russia)

B. SCHULTE[1] AND S. SINDERN[2]
[1]*Philipp-Roeth-Weg 58, 64295 Darmstadt, Germany, (bernd.aloys.schulte@gmx.de)*
[2]*Institut für Mineralogie und Lagerstättenlehre, Rheinisch-Westfälische Technische Hochschule Aachen, 52056 Aachen, Wüllnerstr. 2, Germany*

ABSTRACT Fine grained rodingite-like rocks containing epidote, clinozoisite, garnet, chlorite, phengite and titanite occur within antigorite serpentinite boudins from the high-pressure metamorphic Maksyutovo Complex in the Southern Urals. Pseudomorphs after lawsonite, resorption of garnet by chlorite and phengite and stoichiometry suggest the reaction lawsonite + garnet + K-bearing fluid → clinozoisite + chlorite + phengite, and define a relic assemblage of lawsonite + garnet + chlorite + titanite ± epidote as well as a later post-lawsonite assemblage of clinozoisite + phengite + chlorite + titanite. The reaction lawsonite + titanite → clinozoisite + rutile + pyrophyllite + H_2O delimits the maximum stability of former lawsonite + titanite to pressures > 13 kbar. *P–T* conditions of 18–21 kbar/520–540 °C result, if the average chlorite, Mg-rich garnet rim and average epidote compositions are used as equilibrium compositions of the former lawsonite assemblage. These estimates indicate a similar depth of formation but lower temperatures to those recorded in nearby eclogites. The metamorphic conditions of the lawsonite assemblage are considerably higher than previously suggested and, together with published structural data, support a model in which a normal fault within the Maksyutovo complex acted as the major transport plane of eclogite exhumation.The maximum Si content of phengite and minimum Fe content in clinozoisite constrain the metamorphic conditions of the later pseudomorph assemblage to be > 4.5 kbar and < 440 °C. Rb–Sr isotopic dating of the pseudomorph assemblage results in a formation age of 339 ± 6 and 338 ± 5 Ma, respectively. These results support the recent exhumation models for this complex.

Key words: garnet, lawsonite, Maskyutovo Complex, phengite, rodingite, titanite.

INTRODUCTION

The Maksyutovo Complex in the Southern Urals, Russia, is subdivided into an eclogite facies, structurally lower unit, and a greenschist facies, structurally upper unit (Lennykh, 1977). Serpentinite lenses, up to a kilometre in diameter, occur at the base of the upper unit. They have fine grained centres of epidote, clinozoisite, garnet, chlorite, phengite and titanite. Garnet, epidote, clinozoisite and chlorite are modally dominant and indicate an unusual rock composition rich in Ca and Mg, classified between rodingitic and (ultra)basic. The most spectacular feature of the rock is centimetre sized pseudomorphs after lawsonite which clearly indicate an earlier high-pressure/low-temperature metamorphism (Lennykh & Valizer, 1986). Therefore the rock is defined as a lawsonite fels.

The aim of this paper is to establish the *P–T* conditions of this earlier metamorphism, its relation to the main pseudomorph forming metamorphic event, the age of the pseudomorph formation and the origin of the unusual protolith type. In addition we examine the significance of the relic metamorphism to the tectonometamorphic evolution of the complex.

GEOLOGICAL SETTING

The Maksyutovo Complex of the Central Uralian zone in the Southern Urals formed during Devonian subduction and collision of the continental units of the East European Platform with a Silurian/Devonian island arc (Magnitogorsk island arc, Fig. 1) (Ivanov *et al.*, 1975; Hetzel, 1999). The east-dipping Main Uralian Normal Fault (MUNF) separating the Maksyutovo Complex from the island arc (Fig. 2), is a several kilometres wide mélange zone with serpentinites, basalts, gabbros and various Palaeozoic lithologies. West of the Maksyutovo Complex the Central Uralian zone consists of the greenschist facies Suvanjak Complex, the Upper Devonian Zilair Flysch sedimentary rocks and ophiolitic nappes (Fig. 1). The Maksyutovo Complex is subdivided into two major tectonometamorphic units (Dobretsov *et al.*, 1974; Lennykh *et al.*, 1995; Dobretsov *et al.*, 1996; Hetzel, 1999; Hetzel *et al.*, 1998). The lower unit consists of

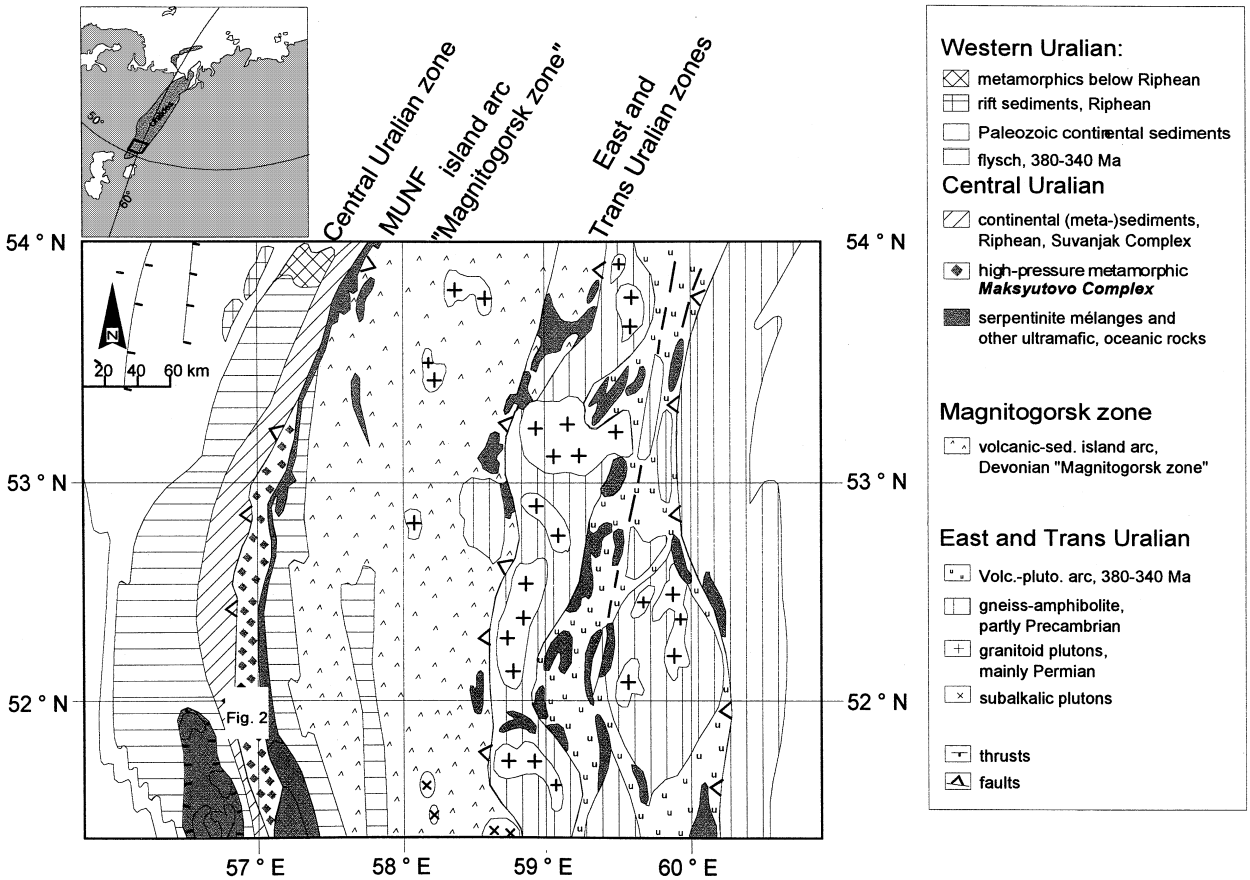

Fig. 1. Southern Urals and the position of the Urals in Eurasia, modified after Lennykh (1977). The position of Fig. 2 is shown in the central Maksyutovo Complex. Inlet shows position of Fig. 1 in Eurasia.

garnet-mica schist, quartzite and local occurrences of eclogite. The upper unit mainly consists of stilpnomelane quartzite. Metabasic greenschist, metachert and a few marble occurrences can be found predominantly close to the base of this unit. Antigorite serpentinite lenses which include the studied lawsonite fels are exclusively present at the base of this unit.

Mineral assemblages of eclogite and garnet-mica schist of the lower unit indicate metamorphic conditions of 550–650 °C and 15–23 kbar (Beane *et al.*, 1995; Lennykh *et al.*, 1995; Dobretsov *et al.*, 1996; Schulte & Blümel, 1999). Isotopic dating of the eclogites using Sm–Nd and Rb–Sr mineral isochrons, U–Pb on rutile and Ar–Ar on phengite gives an age of 385–375 Ma for the eclogite facies metamorphism (Matte *et al.*, 1993; Lennykh *et al.*, 1995; Shatsky *et al.*, 1997; Glodny *et al.*, 1999; Beane & Connelly, 2000). Rb–Sr whole rock and U–Pb zircon dating of eclogites indicate Riphean and Vendian protolith ages (Dobretsov, 1974; Sobolev *et al.*, 1986; Valizer & Lennykh, 1988). The protolith ages and range of lithologies suggest that the lower unit is a relic of the East European passive continental margin (Ivanov *et al.*, 1975 and references therein; Hetzel, 1999 and references therein). The metamorphic conditions of the upper unit are not constrained in detail, but the regional distribution of stilpnomelane + phengite metaclastites (Miyano & Klein, 1989) and metabasites with the assemblage clinozoisite + actinolite + albite + titanite (Frey *et al.*, 1991) indicate greenschist facies conditions. In addition local spessartine quartzites and pumpellyite + chlorite + quartz schists imply temperatures of <400 °C (Coombs *et al.*, 1996; Frey *et al.*, 1991). The pseudomorphs after lawsonite in rodingitized (ultra)mafite (Lennykh & Valizer, 1986) demonstrate that a high-pressure metamorphic event affected at least the serpentinite lenses containing the pseudomorphs. The greenschist facies metamorphism is probably Tournaisian–Viséan in age (Beane, 1997; Beane & Connelly, 2000) and the protolith age of the upper unit is probably Silurian to Ordovician, based on conodont fossils in marbles (Zakharov & Puchkov, 1994). The upper unit is interpreted as a fragment of the palaeo-ocean between the East European platform and the island arc, based mainly on the occurrence of serpentinite and local conodont marble (Ivanov *et al.*, 1975; Dobretsov *et al.*, 1996; Hetzel, 1999).

Structural and regional observations (Echtler & Hetzel, 1997; Puchkov, 1997 and references therein;

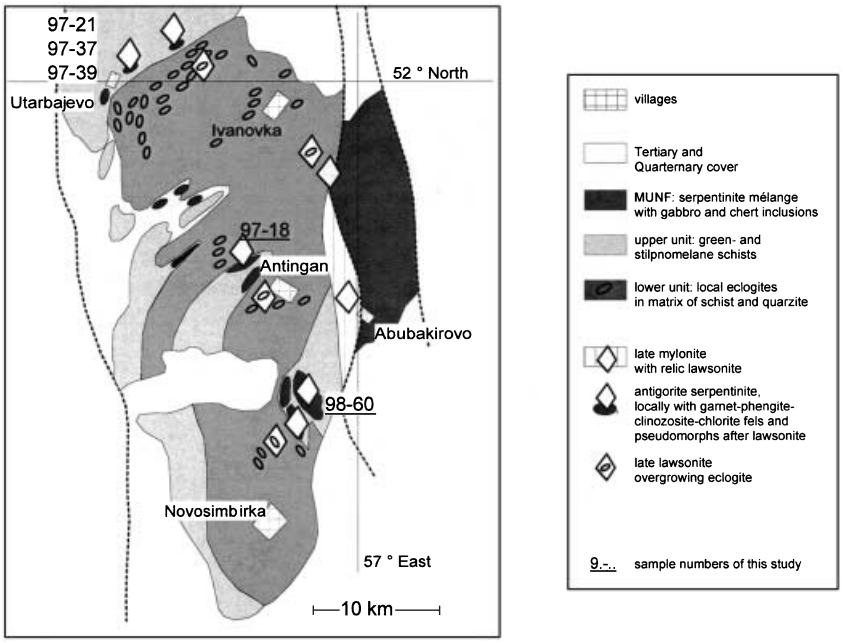

Fig. 2. Simplified geological map of the Central Maksyutovo Complex with samples used in chemical and isotopic analysis, modified after Lennykh (1977).

Hetzel *et al*., 1998) indicate a south-eastward dip of the subduction zone during the eclogite metamorphism. North–south striking structures, defined at map scale, are representative of a later deformation stage at greenschist facies conditions.

FIELD RELATIONS AND PETROGRAPHY

The lawsonite fels occurs as metre scale blocks within the up to kilometre sized antigorite serpentinite boudins (Fig. 2, Table 1). The structural relations between the lawsonite fels and serpentinite are not exposed, but detailed mapping places the lawsonite fels in the centre of the serpentinite boudins (Lennykh & Valizer, 1986) which in turn are rimmed by strongly sheared talc schists, greenschists, marbles, metacherts and stilpnomelane quartzites of the upper unit of the Maksyutovo Complex.

The lawsonite fels consists of centimetre sized, rhombic shaped, bright, polycrystalline aggregates— interpreted as pseudomorphs after lawsonite porphyro- blasts—and a dark matrix (Fig. 3). The pseudomorphs consist of clinozoisite + phengite + garnet + titanite (Fig. 4). The rhombic outline of the pseudomorphs is typical of lawsonite, which is verified by the occurrence of fresh, millimetre sized lawsonite in late, quartzitic mylonite (Fig. 2) and partly pseudomorphosed, relic lawsonite in eclogite (Fig. 2, Lennykh, 1977; Beane *et al*., 1995; Schulte & Blümel, 1999). The dark matrix of the lawsonite fels consists of chlorite + epidote + garnet + titanite ± phengite (Fig. 4).

Table 1. Localities with pseudomorphs after lawsonite in metarodingite.

Latitude	Longitude	Locality	Number	Investigations
51°48,53′	57°53,41′	Novosimbirka	1	
51°49,54′	57°55,15′	Abubakirovo	2	98–60 (*P–T*)
51°53,90′	57°51,42′	Antingan	6	97–18 (age)
51°59,90′	57°45,70′	Utarbajevo	14	97–21, 97–37, 97–39 (age, *P–T*)
52°19,19′	57°47,11′	Maksyutova*	2	
52°22,35′	57°46,44′	Yuldebaevo*	6	

* Not in Fig. 2 but in the north of the Maksyutovo Complex.

Fig. 3. Photograph of metarodingite with rhombic shaped, white pseudomorphs after lawsonite in a dark, chlorite rich matrix. Scale in cm.

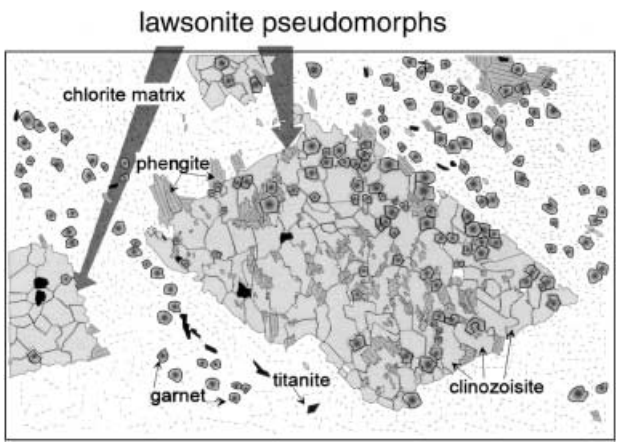

Fig. 4. Thin section sketch of pseudomorph after lawsonite. Length of sketch 1 cm.

Hypidioblastic garnet is surrounded by chlorite in the matrix and, locally, by phengite within the pseudomorphs, indicating partial resorption (Fig. 4). Yellow epidote with metamict core only occurs in the matrix, whereas colourless clinozoisite aggregates are part of the pseudomorphs after lawsonite. Phengite is concentrated along the pseudomorph rim and thus clearly is involved in the lawsonite breakdown reaction. Titanite is the only Ti bearing mineral in the rock and occurs as hypidioblastic grains in the matrix and in the pseudomorphs or as inclusions in the garnet core. Late stage pumpellyite grew in fractures which cut all minerals.

METHODS

Minerals were analysed with an automated CAMECA SX 50 electron microprobe and Rb–Sr isotope ratios were analysed with a FINNIGAN MAT 261 mass spectrometer. For technical data see Appendix. The program THERMOCALC (Powell & Holland, 1988) was used together with the recommended thermodynamic data sets and activity models of Holland & Powell (1996, 1998) for the *P–T* estimates.

MINERAL CHEMISTRY

Garnet in the pseudomorphs and in the matrix has a spessartine-rich core and a spessartine-poor rim (Fig. 5a-f, Table 2) and this zonation is interpreted as a result of prograde metamorphism (Tracy, 1982). There is no difference in zoning style between garnet in the pseudomorphs and in the matrix, but zoning varies between different samples. The zonation in sample 97–39 (Fig 5a,d) is simple, Fe $\leftrightarrow$ Mn in the core and Mn $\leftrightarrow$ Mg in the rim, while Ca is more or less constant throughout the profile. In the garnet core of samples 97–37 (Fig 5b,e) and 98–60 (Fig 5c,f) Mn decreases at the expense of Fe and Ca, while Mg is almost constant and in the garnet rim Fe decreases at the expense of Ca and Mg. The yellow colour of epidote supports the relatively high Fe content analysed, while the colourless clinozoisite has a lower Fe content (Fig. 6, Table 2). An inverse relationship between grossular content in garnet and Fe content in epidote–clinozoisite points to the interdependence between the mineral and rock composition in this multivariant assemblage (compare Figs 5a–f & 6). The phengite and chlorite compositions vary, but no systematic relations are recognised (Figs 7 & 8, Table 2). Titanite only has low Al contents (Table 2) and late pumpellyite is Al-rich with intermediate Fe–Mg ratios (Table 2).

EQUILIBRIUM ESTIMATES AND LAWSONITE-OUT REACTION

The metamict core of epidote indicates long standing radioactivity and therefore either is part of the lawsonite assemblage or even a prelawsonite relic. The resorption of garnet by chlorite and phengite points to the coexistence of former lawsonite with garnet, while phengite and clinozoisite clearly crystallized during the pseudomorph formation. Chlorite is abundant and thus it coexisted with lawsonite and with clinozoisite of the pseudomorphs. The lack of any other Ti-phase beside titanite shows, that titanite also coexisted with lawsonite and clinozoisite. Pumpellyite, filling fractures, is a very late phase, therefore it is not considered further. Thus the petrographic observations indicate two equilibrium assemblages: a former lawsonite assemblage of lawsonite + garnet + chlorite + titanite $\pm$ epidote, and a pseudomorph assemblage of clinozoisite + phengite + chlorite + titanite.

The model system believed to be most applicable to the lawsonite-out reaction is at least trivariant, because there are 10 system components with eight phases (SiO_2, TiO_2, $AlO_{1.5}$, $FeO_{1.5}$, FeO, MgO, MnO, CaO, $KO_{0.5}$, $HO_{0.5}$/lawsonite, fluid, phengite, clinozoisite, garnet, chlorite, titanite, epidote). Therefore three system components have to be reduced if an univariant lawsonite-out reaction is to be written. As Fe, Mg and Mn have similar crystal chemical characteristics they are taken as one component, so the system is reduced to eight components. Although ferric iron occurs in chlorite, phengite and epidote, there is no microprobe means to distinguish between Fe^{2+} and Fe^{3+} and so they combine to a 'mafic component – FFMM', giving a 7×7 Matrix (SiO_2, TiO_2, $AlO_{1.5}$, FFMM, CaO, $KO_{0.5}$, $HO_{0.5}$/aqueous potassium-bearing fluid, phengite, clinozoisite, garnet, chlorite, titanite, epidote) to solve for lawsonite. But the 7×7 matrix is not consistent in that clinozoisite does not coexist with lawsonite. Therefore another approach and further simplification is necessary. Titanite is stable in the lawsonite- as well as in the pseudomorph-assemblage, and thus does not take part in the reaction and may be ignored. Epidote might not have been part of the lawsonite-out reaction because its metamict core possibly implies a prelawsonite growth. Thus the major ferric iron mineral and Fe^{3+} as system component may be omitted. The new matrix – six system components and five phases (SiO_2, $AlO_{1.5}$, 'FMM', CaO, $KO_{0.5}$, $HO_{0.5}$/aqueous potassium-bearing fluid, phengite, clinozoisite, garnet, chlorite) – is not a square matrix. However, a system should be described by the minimum number of necessary system components and in this case K and Si may be combined in the form of a $KSi_{3.3}O_{7.1}$ component indicative of the average K and Si content of phengite giving a 5×5 matrix ($KSi_{3.3}O_{7.1}$, $AlO_{1.5}$, FMM, CaO, $HO_{0.5}$/aqueous-potassium bearing fluid, phengite, clinozoisite, garnet, chlorite) to solve for lawsonite (Table 3). This simplification is believed to be justified, because phengite is the most K and Si rich phase in the system and approximately represents the K and Si concentration of the fluid associated with phengite formation or lawsonite consumption. This in turn means that all other phases—garnet, clinozoisite, chlorite and lawsonite—are free of $KSi_{3.3}O_{7.1}$.

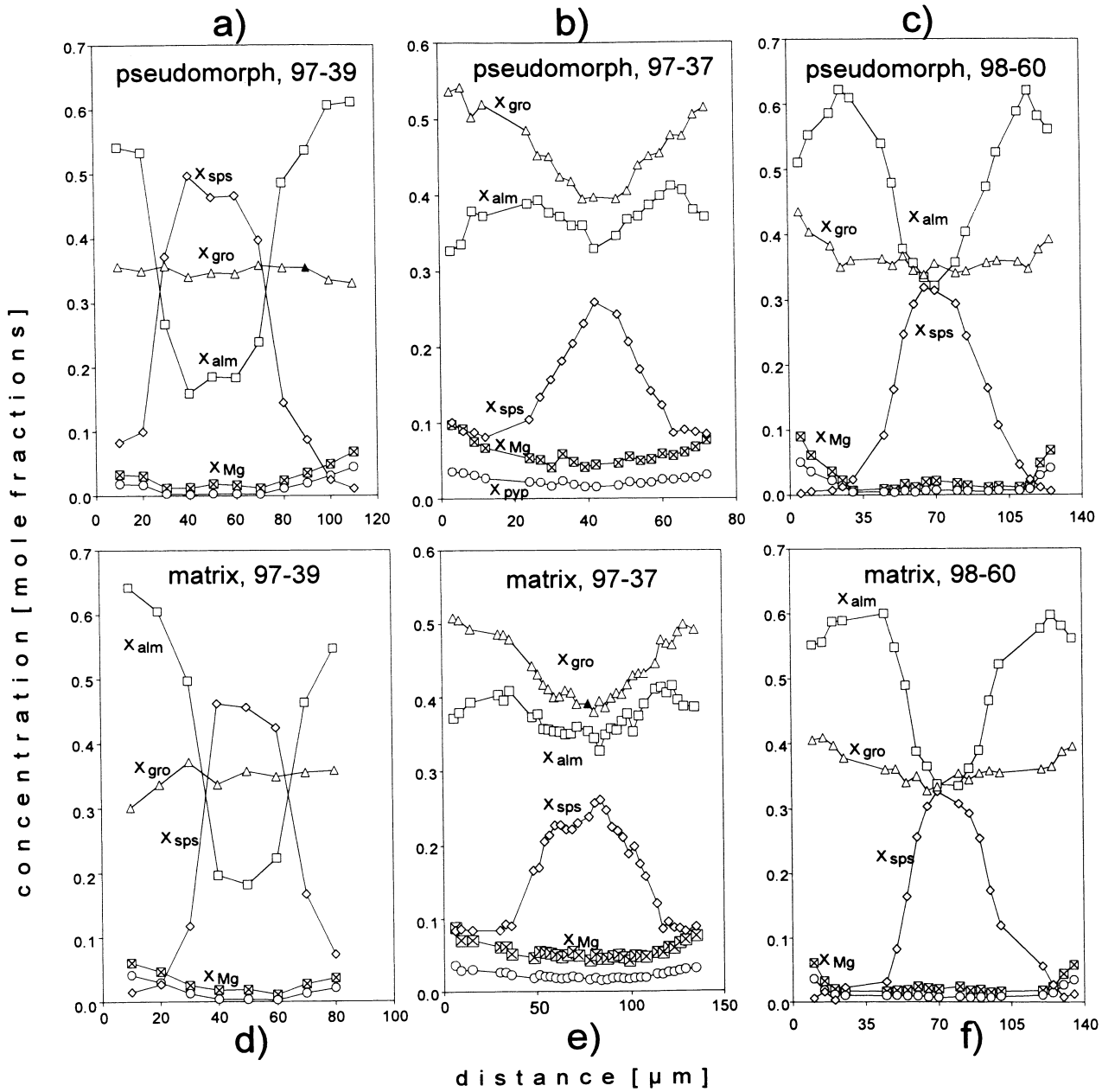

Fig. 5. (a)–(c), garnet compositional zonation in pseudomorphs after lawsonite; (d)–(f), garnet compositional zonation in matrix.

The 5×5 matrix results in

(I): 100 lawsonite + 0.3 garnet + 2 fluid
→ 2 phengite + 50 clinozoisite + 9 chlorite
in sample 97 − 39,

(II): 100 lawsonite + 0.4 garnet + 2 fluid
→ 2 phengite + 50 clinozoisite + 9 chlorite
in sample 97 − 37 and

(III): 100 lawsonite + 0.4 garnet + 2 fluid
→ 2 phengite + 50 clinozoisite + 9 chlorite
in sample 98–60. The stoichiometric relation of 100 lawsonite/0.3–0.4 garnet in reactions (I)–(III) explains the penetrative replacement of lawsonite in contrast to the persistence of garnet.

The system can be graphically displayed in a tetrahedron constructed with the components $AlO_{1.5}$-CaO-(FeO + MgO-MnO)-$KSi_{3.3}O_{7.1}$. The fifth component, $HO0_{.5}$, has to be visualised in a position opposite and central to the $AlO_{1.5}$-CaO-(FeO-MgO-MnO) plane behind the $KSi_{3.3}O_{7.1}$ apex and therefore the $KSi_{3.3}O_{7.1}$-apex represents the fluid composition. Accordingly phengite is projected onto

Table 2. Average compositions of chlorite, clinozoisite and phengite of the pseudomorph assemblage. Garnet rim composition, titanite and epidote of the lawsonite assemblage and average composition of late pumpellyite.

	Epidote			Clinozoisite			Titanite		Garnet		
	97–37	97–39	98–60	97–37	97–39	98–60	97–39		97–37	97–39	98–60
Oxides	10*	15*	8*	7*	25*	22*	8*	Oxides	Rim	Rim	Rim
SiO_2	38.57	38.75	38.48	38.67	38.57	38.51	30.42	SiO_2	37.92	37.16	37.42
TiO_2	0.10	0.07	0.00	0.08	0.18	0.01	39.17	TiO_2	0.07	0.06	0.02
Al_2O_3	31.21	28.72	29.17	32.47	29.65	30.18	1.01	Al_2O_3	21.47	21.76	21.39
Cr_2O_3	0.04	0.04	0.05	0.05	0.03	0.04	0.00	Cr_2O_3	0.04	0.00	0.05
$Fe_2O_3^1$	2.58	6.13	4.92	0.87	4.50	3.82	0.27	FeO[1]	16.94	28.37	24.19
MgO	0.04	0.01	0.01	0.00	0.02	0.01	0.00	MgO	0.93	0.96	1.31
MnO	0.51	0.15	0.39	0.18	0.33	0.58	0.02	MnO	3.77	0.80	0.11
CaO	24.13	24.00	24.33	24.57	24.08	24.51	29.00	CaO	18.03	11.59	15.64
Na_2O	–	–	–	–	–	–	–	Na_2O	–	–	–
K_2O	–	–	–	–	–	–	–	K_2O	–	–	–
Total	97.18	97.87	97.35	96.89	97.36	97.66	99.89	Total	99.17	100.70	100.13
Cations	12.5 O			12.5 O			4 Si	Cations	12 O		
Si	2.98	2.99	2.99	2.98	2.98	2.97	4.00	Si	2.99	2.95	2.96
Ti	0.01	0.00	0.00	0.00	0.01	0.00	3.87	Ti	0.00	0.00	0.00
Al	2.84	2.61	2.67	2.94	2.70	2.75	0.16	Al	2.00	2.04	1.99
Cr	0.00	0.00	0.00	0.00	0.00	0.00	0.00	Cr	0.00	0.00	0.00
Fe^{3+}	0.16	0.39	0.32	0.06	0.29	0.24	0.03	Fe^{2+}	1.12	1.88	1.59
Mg	0.00	0.00	0.00	0.00	0.00	0.00	0.00	Mg	0.11	0.11	0.15
Mn	0.03	0.01	0.03	0.01	0.02	0.04	0.00	Mn	0.25	0.05	0.01
Ca	1.99	1.99	2.02	2.02	2.00	2.03	4.09	Ca	1.53	0.99	1.32
Na	–	–	–	–	–	–	–	Na	–	–	–
K	–	–	–	–	–	–	–	K	–	–	–
Total	8.01	7.99	8.03	8.01	8.00	8.03	12.15	Total	8.00	8.02	8.02
Si + Al + Fe^2	5.98	5.99	5.98	5.98	5.97	5.96		X_{Mg}	0.09	0.06	0.09
Fe/(Fe + Al-1)[2]	0.08	0.20	0.16	0.03	0.14	0.12		Alm	0.37	0.62	0.51
								Prp	0.04	0.04	0.05
								Sps	0.08	0.02	0.00
								Grs	0.51	0.33	0.44

Table 2. (*Cont'd*).

	Chlorite			Phengite			Pumpellyite
	97–37	97–39	98–60	97–37	97–39	98–60	97–37
Oxides	8*	11*	12*	11*	46*	27*	39*
SiO_2	28.94	28.75	28.85	48.81	49.29	49.00	37.58
TiO_2	0.04	0.02	0.05	0.06	0.08	0.05	0.09
Al_2O_3	21.12	20.78	19.96	32.60	31.65	30.39	26.41
Cr_2O_3	0.06	0.03	0.03	0.03	0.04	0.05	0.04
FeO[1]	15.42	22.00	21.91	1.29	1.76	2.48	1.91
MgO	21.79	17.61	17.46	2.03	1.87	2.81	3.40
MnO	0.84	0.57	0.47	0.07	0.04	0.05	1.29
CaO	0.20	0.06	0.10	0.05	0.07	0.06	23.39
Na_2O	0.08	0.03	0.02	0.44	0.33	0.27	0.29
K_2O	0.04	0.03	0.25	10.45	10.27	10.60	0.03
Total	88.53	89.88	89.10	95.83	95.40	95.76	94.43
Cations	14 O			11 O			12.5 O
Si	5.72	5.77	5.85	3.22	3.27	3.26	3.03
Ti	0.01	0.00	0.01	0.00	0.00	0.00	0.01
Al^{IV}	2.28	2.23	2.15	0.78	0.73	0.74	–
Al^{VI}	2.63	2.68	2.62	1.76	1.74	1.65	2.51
Cr	0.01	0.00	0.00	0.00	0.00	0.00	0.00
Fe^{2+}	2.55	3.69	3.71	0.07	0.10	0.14	0.13
Mg	6.42	5.27	5.28	0.20	0.18	0.28	0.41
Mn	0.14	0.10	0.08	0.00	0.00	0.00	0.09
Ca	0.04	0.01	0.02	0.00	0.01	0.00	2.02
Na	0.03	0.01	0.01	0.06	0.04	0.03	0.05
K	0.01	0.01	0.06	0.88	0.87	0.90	0.00
Total	19.84	19.77	19.79	6.97	6.94	7.00	8.25
X_{Mg}	0.72	0.59	0.59	0.74	0.64	0.67	
$y = Al^{IV.}/4$	0.57	0.56	0.54				

* Number of analyses on which mean is based.
Ave = average; X_{Mg} = Mg/(Fe + Mg); Alm = mole fraction of almandine; Prp = mole fraction of pyrope;
Sps = mole fraction of spessartine; Grs = mole fraction of grossular; $Al^{IV.}$ = tetrahedral aluminium; $Al^{VI.}$ = octahedral aluminium.
[1] Total Fe.
[2] Mole fractions.

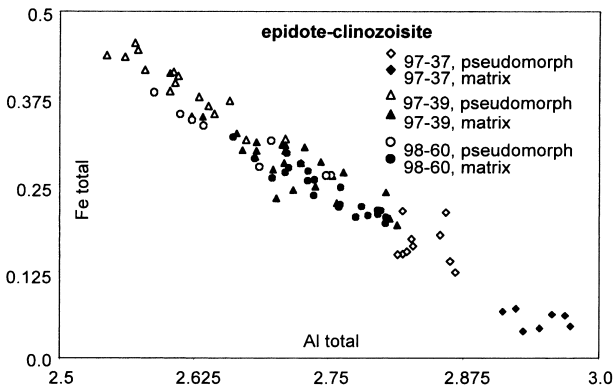

Fig. 6. Fe-Al relationships of epidote-clinozoisite from samples 97–37, 97–39 & 98–60.

the $AlO_{1.5}$-(FeO-MgO-MnO) edge and all other phases plot onto the $AlO_{1.5}$-CaO-(FeO-MgO-MnO) plane (Fig. 9).

In summary, analyses of the petrographic and chemographic data indicate the following four conclusions about the metamorphic evolution: (1) Mg-rich garnet rim + lawsonite + titanite + chlorite (± epidote) define a relic lawsonite assemblage (2) the compositional zonation of garnet implies prograde growth (3) lawsonite broke down by fluid controlled reactions like I–III and (4) chlorite + phengite + clinozoisite + titanite define the pseudomorph assemblage.

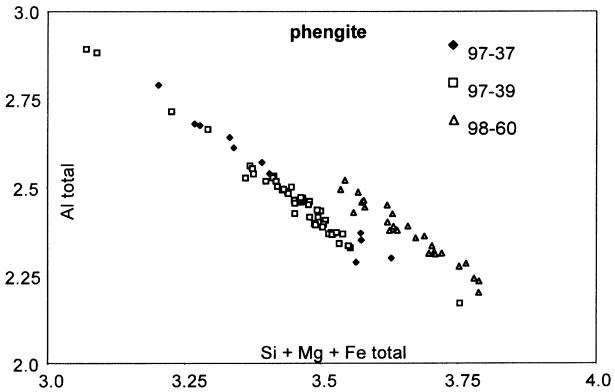

Fig. 7. Phengite $Al_{(tot)}$ v (Si + Mg + $Fe_{(tot)}$) composition in samples 97–37, 97–39 & 98–60.

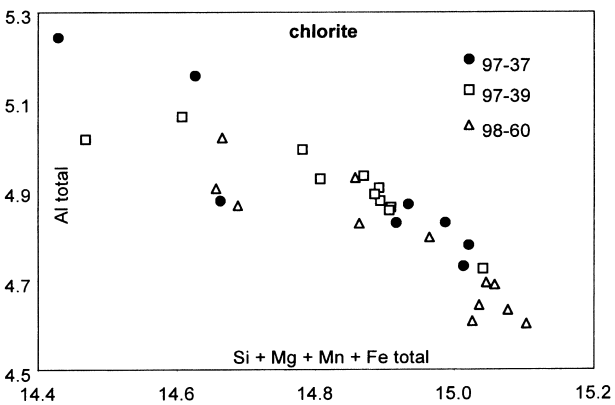

Fig. 8. Al v (Si + Mg + Fe + Mn) of chlorite from samples 97–37, 97–39 & 98–60.

Table 3. A 5 × 5 matrix to solve for lawsonite.

	grt	phg	chl	czo	fluid	lws
$KSi_{3.3}O_{7.1}$	0	1	0	0	1	0
$AlO_{1.5}$	2	2.4	4.9	3	0	2
CaO	1.5–1*	0	0	2	0	1
FeMgMnO	2–1.5*	0.3	9	0	0	0
H_2O	0	1	16	1	1	1

* Depends on sample, all other values are average or ideal values.

PRESSURE AND TEMPERATURE ESTIMATES

Lawsonite assemblage

The maximum stability of lawsonite + titanite is given by reaction

(IV) lawsonite + titanite → clinozoisite + rutile + pyrophyllite + H_2O.

Different clinozoisite compositions ($X_{epidote}$ = 0–0.5) were used to simulate the epidote component. Within this compositional range the reaction is stable up to 30 kbar and more. The most Fe-rich clinozoisite in the pseudomorphs of each sample delimits the maximum stability of the former lawsonite and titanite coexistence to temperatures < 400 °C at 10 kbar and < 580 °C at 20 kbar (Fig. 10a).

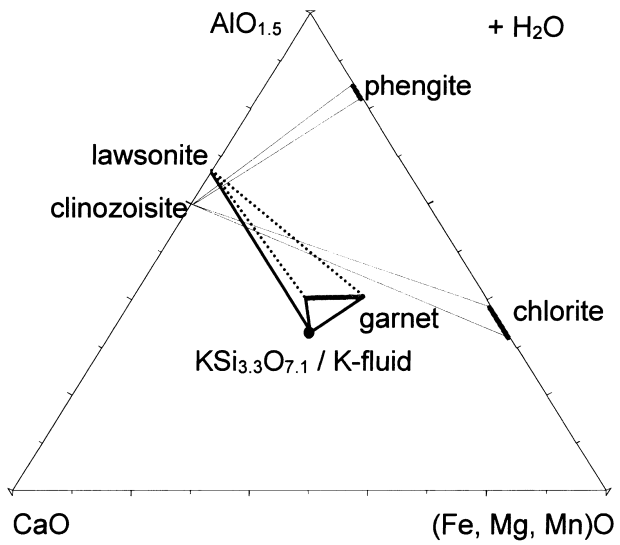

Fig. 9. Al-Ca-(Fe^{2+} + Mg + Mn) diagram, projected from $KSi_{3.3}O_{7.1}$ and H_2O: Garnet-lawsonite tie line crosscuts clinozoisite-chlorite tie line. The phengite projection plots on the $AlO_{1.5}$-(FMM)O side and the fluid is placed in the centre of the triangle.

The *P–T* conditions of the lawsonite assemblage may be constrained further: the six system components CaO-MgO-FeO-$AlO_{1.5}$-SiO_2-$HO_{0.5}$ with the four phases, garnet rim + lawsonite + chlorite + H_2O is a good approximation to the real system, because phengite was not present in the lawsonite assemblage. Titanite may be omitted because it is the only Ti-phase. As the spessartine content in garnet is low (1–8 mole%) and probably mixes in close to ideal conditions with almandine it is added to the almandine component. A minimum temperature of > 460 °C at minimum pressures of > 13 kbar is estimated for the quadrivalent assemblage garnet rim + lawsonite + chlorite (of any composition) + H_2O (Fig. 10a). This estimate takes into account, that neither the exact chlorite composition, nor the coexistence of epidote in the lawsonite assemblage is known.

In order to derive a *P–T* estimate it is necessary to make three assumptions namely that: (i) epidote is part of the lawsonite assemblage and (ii) chlorite and (iii) epidote compositions in the lawsonite assemblage are specified. Chlorite is modally abundant and thus it's composition in the lawsonite assemblage might be similar to the existing composition. Epidote is quite resistant to re-equilibration (Franz & Selverstone, 1992) and thus its composition might also be unchanged. However, no systematic relations are recognised for chlorite and epidote compositions and therefore the existing average values are used for

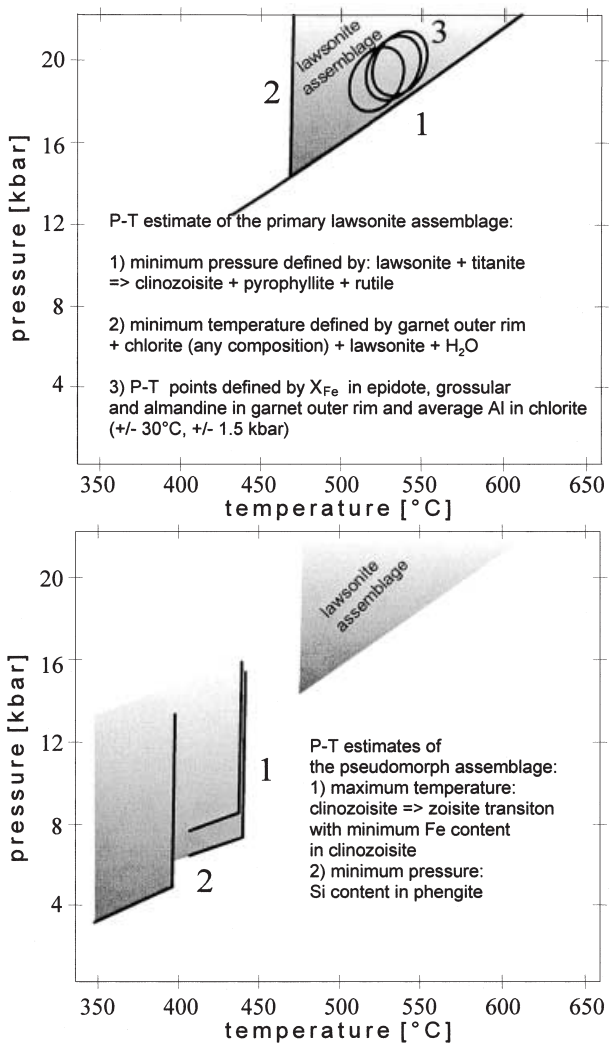

Fig. 10. (a)–(b). (a) Stability of the lawsonite assemblage is defined by maximum stability of lawsonite + titanite and the minimum stability of garnet + chlorite + lawsonite + H_2O. Additional estimates, shown by ovals are based on average chlorite and epidote compositions (see Table 4). (b) Maximum stability of the pseudomorph assemblage is defined by the clinozoisite = > zoisite transition with minimum Fe content in clinozoisite and by maximum Si content in phengite.

the *P–T* calculation. Now seven system components with five phases (CaO-FeO-Fe_2O_3-MgO-$AlO_{1.5}$-SiO_2-$HO_{0.5}$/garnet, chlorite, lawsonite, epidote, H_2O) indicate again quadrivalency and the four phase components grossular, almandine, $X_{epidote}$ (Fe/(Fe + Al-1) and $y_{chlorite}$ (Al^{IV}/4) have to be fixed. Using the garnet rim, average chlorite and epidote compositions for samples 97–37, 97–39 and 98–60 (Table 4, Fig. 10a) estimates of 20.3 kbar/540 °C, 18.3 kbar/518 °C and 20.7 kbar/543 °C are derived.

In summary, despite the unknown equilibrium composition of chlorite and epidote and the uncertainty if epidote coexisted with lawsonite, the *P–T* calculations reveal that the assemblage was formed at pressures > 13 kbar and temperatures between 460 and 550 °C. The lack of any indication for pressure as high as 13 kbar in the upper unit of the Maksyutovo Complex leads to the interpretation that the serpentinite lenses containing the pseudomorphs after lawsonite were incorporated into the base of the upper unit subsequent to high-pressure metamorphism.

Table 4. Mineral compositions used to estimate *P–T* of lawsonite and pseudomorph assemblage.

Sample	97–37	97–39	98–60
lawsonite assemblage			
almandine + spessartine (outer rim)	0.45	0.63	0.51
grossular (outer rim)	0.51	0.33	0.45
average X_{Fe} epidote = (Xep)	0.08	0.2	0.16
average Al^{IV}/4 chlorite = y(chl)	0.57	0.56	0.54
P (kbar)	20.3	18.3	20.7
T (°C)	540	518	543
pseudomorph assemblage			
X_{Fe} minimum clinozoisite	0.02	0.1	0.1
Si p.f.u. maximum phengite	3.27	3.44	3.36
minimum pressure (kbar)	> 4.5	> 7.5	> 6.0
maximum temperature (°C)	< 386	< 433	< 433

Pseudomorph assemblage

Any precise estimate of *P–T* conditions of the pseudomorph assemblage clinozoisite + phengite + chlorite + H_2O is strongly hampered by the variability of mineral compositions and the unknown Fe^{3+} content in phengite and chlorite. However, maximum temperatures may be derived from the clinozoisite to zoisite transition using the minimum Fe content in clinozoisite (Holland & Powell, 1998), and minimum pressures from the highest Si content in phengite (Massone, 1991; Massonne & Schreyer, 1987). For samples 97–37, 98–60 and 97–39 the derived values are > 4.5 kbar/< 400 °C, > 6 kbar/< 440 °C, and > 7.5 kbar/ < 440 °C, respectively (Table 4, Fig. 10b). The temperature of the pseudomorph formation is obviously lower than that of the lawsonite assemblage, indicating that the pseudomorph-forming event was not isofacial with the lawsonite assemblage. The minimum pressure for the pseudomorph assemblage is near or above the maximum pressure stability of stilpnomelane + phengite in metasiliclastic rocks (Miyano & Klein, 1989), indicating that the pseudomorph formed during exhumation. Assuming that the upper unit never reached depths greater than those defined by the stilpnomelane stability field (see above; Fig. 12), it is concluded that the pseudomorph formed prior to incorporation of the pseudomorph-containing-serpentinite lenses into the base of the upper unit.

Rb–Sr dating

For samples 97–18 and 97–21, fractions of all modal components have been used for isotopic analyses using the Rb–Sr system (Table 5), which is

appropriate for dating the pseudomorphs that are modally dominated by clinozoisite + phengite. Both samples have Sr concentrations that are low in the matrix (70 and 134 p p m) and high in the pseudomorphs (2987 and 3440 p p m). The Rb concentrations and Rb/Sr ratios are generally rather low, except for white mica (Table 5). In addition pseudomorphs of metarodingites from the north of the Maksyutovo Complex (sample 97–3) also show these Rb/Sr characteristics (Table 5) which seems to be a regional phenomenon (see Discussion). The breakdown of the lawsonite porphyroblasts by the fluid-controlled reaction (I)– (III) explains the cogenetic origin of clinozoisite and phengite as indicated by the textural observations. Thus the isotopic data from these two minerals were used for isochron calculation (Table 5, Fig. 11) and the two samples yield ages of 339 ± 6 and 338 ± 5 Ma, which are identical within error. The $^{87}Sr/^{86}Sr$ – $^{87}Rb/^{86}Sr$ ratio of garnet in sample 97–18, within its limits of error, lies on the isochron although garnet – at least the core – is not part of the pseudomorph forming assemblage. This indicates either that the garnet + lawsonite assemblage did not differ isotopically in a significant way from the pseudomorph assemblage, or that garnet equilibrated isotopically with clinozoisite and phengite.

Two matrix parts from sample 97–18 have markedly different Rb/Sr isotope signatures (Fig. 11) and deviate from the isochron of the pseudomorph components. Comparing these data with those from the matrix of sample 97–21 indicates that the isotopic heterogeneity in the matrix of 97–18 is best explained by an episodic loss of Rb in various parts of the matrix during different stages of the isochron development after initial equilibration at *c*. 339 Ma. This might have caused a shift from a position with high $^{87}Rb/^{86}Sr$-ratio on the isochron to one with lower $^{87}Rb/^{86}Sr$ ratios above the isochron.

Table 5. Rb–Sr isotope data of pseudomorphs after lawsonite.

	$Rb_{(p.p.m.)}$	$Sr_{(p.p.m.)}$	$^{87}Rb/^{86}Sr$	$^{87}Sr/^{86}Sr$
sample 97–18				
phengite*	224	150	4.33 ± 0.05	0.72909 ± 0.00005
c-zoisite*	1.4	5289	0.00078 ± 0.00002	0.70822 ± 0.00005
garnet	0.3	29	0.031 ± 0.0007	0.70832 ± 0.00005
pseudom.	12	3540	0.0096 ± 0.0001	0.70821 ± 0.00005
matrix 1	1	134	0.0115 ± 0.0002	0.70850 ± 0.00005
matrix 2	0.2	110	0.004 ± 0.0015	0.70835 ± 0.00005
isochron	age(Ma)	$^{87}Sr/^{86}Sr$		
calculation	339 ± 6	initial:		0.70822 ± 0.00005
sample 97–21				
phengite*	109	170	1.86 ± 0.02	0.71787 ± 0.00005
c-zoisite*	5	3539	0.0042 ± 0.0001	0.70895 ± 0.00005
pseudom.	28	2987	0.0274 ± 0.0003	0.70908 ± 0.00005
matrix	1	70	0.0612 ± 0.0014	0.70919 ± 0.00005
isochron	age(Ma)	$^{87}Sr/^{86}Sr$		
calculation	338 ± 5	inital:		0.70893 ± 0.00005
sample 97–3				
pseudomorph	26	3340	0.0222 ± 0.0003	0.70936 ± 0.00005

* Used for isochron calculation sample 97–18.

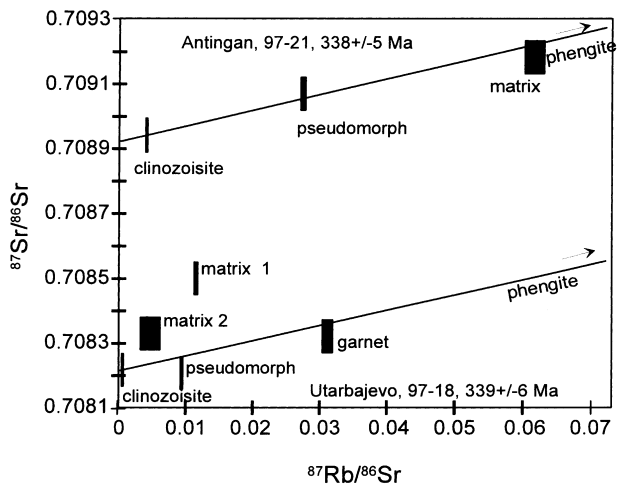

Fig. 11. $^{87}Rb/^{86}Sr$-$^{87}Sr/^{86}Sr$-isochron diagram for samples 97–18 and 97–21. The size of symbols indicates 2σ errors of the analyses.

DISCUSSION

Lawsonite assemblage, rock composition

The deduction of the lawsonite assemblage is based on garnet resorption by chlorite and phengite and the stoichiometry of reaction (I)–(III). In addition Fe-Mg exchange between garnet/chlorite and garnet/phengite gives temperatures of < 350 °C, which are interpreted as disequilibrium, because garnet with up to 5 mole percentage pyrope and 1 mole percentage spessartine is not stable at < 350 °C, at least in Si saturated compositions (Mahar *et al*., 1997). Another indicator of the coexistence of garnet + lawsonite is that the decomposition of lawsonite to clinozoisite is always associated with grossular on the lawsonite side in a CASH system with grossular, lawsonite, pyrophyllite, kyanite, margarite, anorthite, laumontite, that is a simplified model for rocks of rodingitic composition at subgreenschist to blueschist facies conditions. Lawsonite coexisting with garnet is described in various rocks at different high-pressure metamorphic conditions (Black, 1977; Caron & Pecquinot, 1986; Okay, 1980; Helmstaedt & Schulze, 1988). However, it is a rare assemblage that is restricted to geological settings with very low temperature gradients and lithologies rich in Ca and Al.

Rodingites are metasomatic rocks rich in Ca-Al-silicate minerals and are commonly associated with serpentinites. They occur at contacts between serpentinite and country rock or as dykes, sills and boudins within serpentinite (Bloxam, 1955; Bilgrami & Howie, 1960; Dubinska, 1995; O'Hanley *et al*., 1992) as do the presently described rocks. Rodingites mostly derive from mafic rocks (e.g. gabbro, diabase) but sedimentary protoliths have also been described (Rice, 1983).

Table 6. Rock Composition of sample 97–39 from Utarbajewo (oxide wt%).

SiO_2	TiO_2	Al_2O_3	Fe_2O_3	MnO	MgO	CaO	Na_2O	K_2O	P_2O_5	S
35.3	1.39	24.4	14.7	1.31	6.48	11.2	0.12	1.19	0.01	< 0.02

The rodingitization of the mafic rocks and the serpentinization of the ultramafic rocks are probably cogenetic processes (Schandl *et al.*, 1989; Thayer, 1966) that lead to the addition of Ca, Al, OH- and removal of Si and alkalis (Na, K) from the mafic rocks (Harper *et al.*, 1988; Staudigel *et al.*, 1981). Rodingites are known from oceanic fracture zones (Honnorez & Kirst, 1975) as well as in re-equilibrated rocks in alpine-type ophiolites (e.g. Deutsch, 1979; Evans *et al.*, 1979; Evans *et al.*, 1981; Rösli *et al.*, 1991). In all the settings there is a wide range of rock compositions (SiO_2: 52–33 wt%, Al_2O_3: 10–25 wt%, CaO: 20–30 wt%, rest: < 37 wt%). Sample 97–39 plots within the published range of (meta-)rodingite compositions, except for CaO (CaO = 11.2 wt%) (Table 6), and so is better termed as a rodingitized (ultra)mafic rock, rather than a (meta)rodingite.

Pseudomorph formation

The pseudomorph assemblage formed by the infiltration of a K-bearing fluid into the rock via reactions (I)-(III) and the Rb–Sr ages are interpreted to date the isotopic equilibration between the pseudomorph minerals clinozoisite and phengite. In principle, the isotopic equilibration between clinozoisite and phengite could also have occurred after the formation of the pseudomorphs due to subsequent heating or an influx of fluids, but the following two lines of evidence suggest that this is not the case. First, the temperature in the pseudomorphs did not exceed 440 °C (see *P–T* estimate), and so re-equilibration due to heating seems unlikely. Second, Rb–Sr ages obtained from mylonites, quartzites and mica schist in the central Maksyutovo Complex cluster at *c.* 360 Ma (Beane & Connelly, 2000) and preclude a regional resetting of the Rb–Sr system by fluids at 339–338 Ma. In consequence, it is most plausible that the isotopic equilibration dates the crystallization of the pseudomorph minerals at a point between the $^{40}Ar/^{39}Ar$ ages of 338–331 Ma from phengite of the upper unit and 365–358 Ma from phengite of the lower unit (Beane & Connelly, 2000). The high Sr concentrations and low $^{87}Rb/^{86}Sr$ ratios of the pseudomorphs raise the question if they are products of a crystallization event at 339–338 Ma, or whether they are features of the precursor lawsonite. If the former was true, the regional occurrence of the high Sr concentrations in the lawsonite fels would require an influx of appreciable amounts of Sr and probably elements with similar transport characteristics such as Ca, Eu or Ba for which there is no evidence. Extremely low $^{87}Rb/^{86}Sr$ ratios and high Sr concentrations of more than 1400 p p m are characteristic of lawsonite (Domanik *et al.*, 1993; Miyajima *et al.*, 1999). It is thus probable that the Rb–Sr characteristics of the pseudomorphs are inherited from the precursor lawsonite and that the fluid, responsible for lawsonite break-down, was not Sr rich. The exact origin of the fluid remains obscure so far, but it seems obvious, that the normal fault between the lower unit and upper unit may have triggered the fluid influx and the abundance of metasiliclastic rocks in both units is a potential source for the K-bearing fluid.

Tectonometamorphic significance

Pressures of > 13 kbar and temperatures of < 550 °C are estimated for the lawsonite assemblage, which is a similar pressure but lower temperature to the eclogites of the lower unit (Beane *et al.*, 1995; Dobretsov *et al.*, 1996; Schulte & Blümel, 1999). The same relationship is also recognised if the lawsonite + titanite stability of the lawsonite fels is compared with the lawsonite + jadeite stability of the eclogites (Fig. 12). Both stabilities have a similar slope and values in *P–T* space, but the lawsonite + jadeite formation in eclogite is a late process that post-dates the peak metamorphic temperatures (Beane *et al.*, 1995; Lennykh *et al.*, 1995;

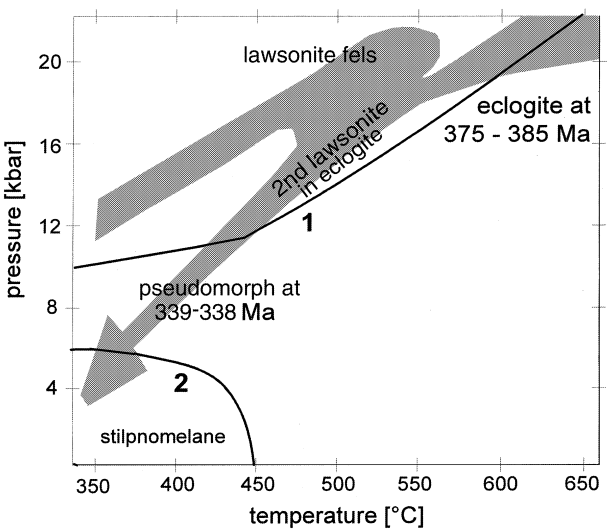

Fig. 12. (1) Stability of secondary lawsonite in eclogite in lower unit and stilpnomelane metaclastites in upper unit. Stability of lawsonite is limited by the reactions lawsonite + jadeite ($X_{jd} = 0.43$) => clinozoisite ($X_{Fe} = 0.5$) + paragonite and jadeite ($X_{jd} = 0.43$) + quartz => albite. (2) Stability of stilpnomelane after Miyano & Klein (1989).(3) P–T-t path interpretation of the lawsonite fels and eclogite. Oceanic and continental crust, represented by lawsonite fels and eclogite of the lower unit meet at a minimum of 13 kbar/470 °C, are exhumed together and partially re-equilibrate in the stability field of stilpnomelane. The formation of the lawsonite fels predates 339 Ma and post-dates the formation of eclogites (375–385 Ma, Matte *et al.*, 1993; Shatsky *et al.*, 1997).

Schulte & Blümel, 1999), whereas the lawsonite + titanite stability characterises the peak metamorphic conditions of the lawsonite fels. It is noted that thermal modelling and field studies of subduction settings (Peacock, 1993; Ernst & Peacock, 1996; Trouw *et al*., 1998) also show strong temperature variations with 'cold' margins and 'hot' centres in an horizontal section through a subduction zone. Thus the present distribution of 'high temperature eclogite' and 'low temperature lawsonite fels' in the central Maksyutovo Complex (Fig. 2) resembles such a horizontal section through a relic south-east dipping subduction zone and might have persisted further transposition and re-equilibration.

The ultramafic rocks with lawsonite fels are boudins with undeformed cores and strongly foliated rims, which can be attributed to rigid, exotic blocks, within fault zones. This type of structural arrangement can be interpreted as the boudins being constitutional parts of the fault zone at the base of the upper unit that separates the lower from the upper unit (Dobretsov *et al*., 1996; Hetzel *et al*., 1998; Leech & Ernst, 2000). If this is correct then it indicates (1) the width of the fault zone between the lower unit and the upper unit increases upwards (2) the close association of ultramafic rock, lawsonite fels, marble and metachert, and thus all rocks with 'oceanic affinity', are part of this normal fault (3) the derived *P–T* estimate of the lawsonite fels demonstrates that this fault zone became active at low-temperature eclogite facies conditions and (4) the upper unit is not necessarily of oceanic origin but restricted to the greenschist facies metamorphosed stilpnomelane-phengite metaclastites. These conclusions strongly support the exhumation model of Hetzel *et al*. (1998), that stresses the significance of this internal normal fault zone in the Maksyutovo Complex as a major transport plane of exhumation for the eclogites.

CONCLUSIONS

The eclogite facies lower unit of the Maksyutovo Complex is separated by a normal fault zone from the greenschist facies upper unit. Included in the fault zone are ultramafic boudins that enclose blocks of lawsonite fels. The *P–T* estimate of the assemblage lawsonite + titanite + garnet + chlorite ± epidote in this rock points to similar depths but lower temperatures of formation as the eclogites of the lower unit (Fig. 12). This pressure estimate suggests that the fault zone was active at low-temperature eclogite facies conditions and supports the significance of the fault zone as a major plane of eclogite exhumation (Hetzel *et al*., 1998). The *P–T* conditions and age (339–338 Ma) of the pseudomorph formation either correlate with the greenschist facies metamorphism in the upper unit or with a late exhumation stage of the lower unit, respectively, the activity of the normal fault zone.

ACKNOWLEDGEMENTS

Our thanks to V. I. Lennykh for two excellent field trips through the Maksyutovo Complex and fruitful discussions in the summers of 1997 and 1998. Additionally we thank the reviewers and the editor for constructive criticism, P. Blümel (TU Darmstadt), U. Kramm, A. Rogers (RWTH Aachen) and A. Willner (Ruhr-University Bochum) for discussions on the subject and K. Richter (University Würzburg) and H. Ortner (TU Darmstadt) who provided analytical facilities. We are grateful to U. Haack and J. Schneider (University Gießen) who made the isotope analyses possible. J. Kolb and B. Thybusch (TU Darmstadt) prepared samples and helped during analytical work. Most of this study was financed by the Deutsche Forschungs Gemeinschaft.

REFERENCES

Beane, R. J., 1997. Ar/Ar evidence for Paleozoic high-pressure metamorphism in the South Urals. In: *Annual Meeting of the Geological Society of America, (EOS EI)* (Suppl.) Salt Lake City, pp. BTH-35.

Beane, R. J. & Connelly, J. N., 2000. $^{40}Ar/^{39}Ar$, U-Pb, and Sm-Nd constraints on the timing of metamorphic events in the Maksyutov Complex, southern Ural Mountains. *Journal of the Geological Society of London*, **157,** 811–822.

Beane, R. J., Liou, J. G., Coleman, R. G. & Leech, M. L., 1995. Petrology and retrograde *P-T* path for eclogites of the Maksyutov Complex, South Ural Mountains, Russia. *Island Arc*, **4,** 254–266.

Bilgrami, S. A. & Howie, R. A., 1960. The Mineralogy and the Petrology of a Rodingite Dike, Hindubagh, Pakistan. *American Mineralogist*, **45,** 791–801.

Birck, J. L. & Allègre, C. J., 1978. Chronology and chemical history of the parent body of basaltic achondrites studied by the $^{87}Rb/^{86}Sr$ method. *Earth and Planetary Science Letters*, **39,** 37–51.

Black, P. A. M., 1977. Regional high-pressure metamorphism in New Caledonia: Phase equilibria in the Ouéga district. *Tectonophysics*, **43,** 59–107.

Bloxam, T. W., 1955. Rodingite from the Girvan-Ballantrae complex, Ayrshire. *Mineralogical Magazine*, **30,** 525–528.

Caron, J. M. & Pecquinot, G., 1986. The transition between blueschists and lawsonite-bearing eclogites based on observations from Corsican metabasalts. *Lithos*, **19,** 205–218.

Coombs, D. S., Kawachi, Y. & Ford, B. P., 1996. Porphyroblastic manganaxinite metapelagites with incipent garnet in prehnite-pumpellyite facies, near Meyers Pass, Torless Terrane, New Zealand. *Journal of Metamorphic Geology*, **14,** 125–142.

Deutsch, A., 1979. Serpentinite und Rodingite der Cima Sgiu (NW Aduladecke, Ticino). *Schweizerische Mineralogische Petrographische Mitteilungen*, **59,** 319–347.

Dobretsov, N. L., 1974. *Glaucophane Schists and. Eclogite-Glaucophane-Schist complexes in the USSR*. Nauka press, Novosibirsk (in Russian).

Dobretsov, N. L., Shatsky, V. S., Coleman, R. G., Lennykh, V. I., Valizer, P. M., Liou, J., Zhang, R. & Beane, R. J., 1996. Tectonic setting and Petrology of Ultrahigh-Pressure Metamorphic Rocks in the Maksyutov Complex, Ural Mountains, Russia. *International Geology Review*, **38,** 136–160.

Dobretsov, N. L., Sobolev, V. S., Sobolev, N. V. & Khlestov, V. V., 1974. *The Facies of Regional Metamorphism at High pressure*. Moscov (English Translation by DA Brown 1975. ANU Press, Canberra.

Domanik, K. J., Hervig, R. L. & Peacock, S. M., 1993. Beryllium and boron in subduction zone minerals: An ion microprobe study. *Geochimica et Cosmochimica Acta*, **57,** 4997–5010.

Dubinska, E., 1995. Rodingites of the Eastern Part of the Jordanów – Gogolów Serpentinite Massif, Lower Silesia, Poland. *Canadian Mineralogist*, **33,** 585–608.

Echtler, H. P. & Hetzel, R., 1997. Main Uralian Thrust and Main Uralian Normal Fault: non-extensional Paleozoic high-P rock exhumation, oblique collision, and normal faulting in the Southern Urals. *Terra Nova*, **9,** 158–162.

Ernst, W. G. & Peacock, S. M., 1996. A thermotectonic model for preservation of ultrahigh-pressure phases in metamorphosed continental crust. In: *Subduction, Top to Bottom*. (eds Bebout, G. E., Scholl, D. W., Kirby, S. H. & Platt, J. P.) *Geophysical Monograph*. 96, 171–178.

Evans, B. W., Trommsdorf, V. & Goles, G. G., 1981. Geochemistry of High-Grade Eclogites and Metarodingites from the Central Alps. *Contributions to Mineralogy and Petrology*, **76,** 301–311.

Evans, B. W., Trommsdorf, V. & Richter, W., 1979. Petrology of an eclogite-metarodingite suite at Cima di Gagnone, Ticino, Switzerland. *American Mineralogist*, **64,** 15–31.

Franz, G. & Selverstone, J., 1992. An empirical phase diagram for the clinozoisite-zoisite transformation in the system $Ca_2Al_3Si_3O_{12}$ (OH)-$Ca_2Al_2Fe^{3+}Si_3O_{12}$ (OH). *American Mineralogist*, **77,** 631–642.

Frey, M., de Capitani, C. & Liou, J. G., 1991. A new petrogenetic grid for low-grade metabasites. *Journal of Metamorphic Geology*, **9,** 497–509.

Glodny, J., Austrheim, H., Bingen, B., Rusin, A. & Scarrow, J. H., 1999. New age data for high-P rocks and ophiolites along the Main Uralian Fault, Urals, Russia: Implications for the Uralian orogeny. *Terra Nostra*, **99/1,** 89–90.

Harper, G. D., Bowman, J. R. & Kuhns, R., 1988. A Field, Chemical and Stable Isotope Study of Subseafloor Metamorphism of the Josephine Ophiolite, California-Oregon. *Journal of Geophysical Research*, **93,** 4625–4656.

Helmstaedt, H. & Schulze, D. J., 1988. Eclogite facies ultramafic xenoliths from Colorado Plateau diatreme breccias: Comparison with eclogites in crustal environments, evaluation of the subduction zone hypothesis and implications for eclogite xenoliths from Diamandoferous kimberlites. In: *Eclogites and Eclogite Facies Rocks* (ed. Smith, D.C.), 387–450 Elsevier, New York.

Hetzel, R., 1999. Geology and geodynamic evolution of the high-pressure/low-temperature metamorphic Maksyutov Complex, Southern Urals, Russia. *Geologische Rundschau*, **87,** 577–588.

Hetzel, R., Echtler, H. P., Seifert, W., Schulte, B. A. & Ivanov, K. S., 1998. Subduction- and exhumation-related fabrics in the Paleozoic high-pressure/low-temperature Maksyutov complex, Antingan area, Southern Urals, Russia. *Geological Society of America Bulletin*, **110,** 916–930.

Holland, T. J. B. & Powell, R., 1996. Thermodynamics of order-disorder in minerals. II. Symmetric formalism applied to solid solutions. *American Mineralogist*, **81,** 1425–1437.

Holland, T. J. B. & Powell, R., 1998. An internally consistent thermodynamic data set for phases of petrological interest. *Journal of Metamorphic Geology*, **16,** 309–343.

Honnorez, J. & Kirst, P., 1975. Petrology of Rodingites from the Equatorial Mid-Atlantic Fracture Zones and Their Geotectonic Significance. *Contributions to Mineralogy and Petrology*, **49,** 233–257.

Ivanov, S. N., Perfiliev, A. S., Efimov, A. A., Smirnov, G. A., Necheukhin, V. M. & Fershtater, G. B., 1975. Fundamental features in the structure and evolution of the Urals. *American Journal of Science*, **254A,** 107–136.

Leech, M. L. & Ernst, W. G., 2000. Petrotectonic evolution of the high- to ultrahigh-pressure Maksyutov Complex, Karayanova area, south Ural Mountains: structural and oxygen isotopic constraints. *Lithos*, **52,** 235–252.

Lennykh, V. I., 1977. Eclogite–glaucophaneschist of the South Urals. Akademii Nauka, Moskau (in Russian).

Lennykh, V. I. & Valizer, P. M., 1986. Lawsonite rodingite of the Maksyutov eclogite–glaucophane complex. Sverdlovsk, Nauka Press, 73–76 (in Russian).

Lennykh, V. I., Valizer, P. M., Beane, R. J., Leech, M. & Ernst, W. G., 1995. Petrotectonic Evolution of the Maksyutov Complex, Southern Urals, Russia: Implications for Ultrahigh-Pressure Metamorphism. *International Geology Review*, **37,** 584–600.

Mahar, E. M., Baker, J. M., Powell, R., Holland, T. J. B. & Howell, N., 1997. The effect of Mn on mineral stability in metapelites. *Journal of Metamorphic Geology*, **15,** 223–238.

Massone, H. J., 1991. *High-Pressure, Low-Temperature Metamorphism of Pelitic and Other Protoliths Based on Experiments in the System* K_2O-MgO-Al_2O_3-Sio_2-H_2O Unpublished Habilitation, Ruhr-Universität Bochum, Germany.

Massonne, H. J. & Schreyer, W., 1987. Phengite geobarometry based on the limiting assemblage with K-feldspar, phlogopite, and quartz. *Contributions to Mineralogy and Petrology*, **96,** 212–224.

Matte, P., Maluski, H., Caby, R., Nicolas, A., Kepezhinskas, P. & Sobolev, S., 1993. Geodynamic model and Ar/Ar dating for the generation and emplacement of the High Pressure (HP) metamorphic rocks in SW Urals. *Comptée Rendue Academie Science*. **317/ II,** 1667–1674.

Miyajima, H., Matsubara, S., Miyawaki, R. & Ito, K., 1999. Itoigawaite, a new mineral, the Sr-analogue of lawsonite in jadeitite from the Itoigawa-Ohmi district, central Japan. *Mineralogical Magazine*, **63,** 909–916.

Miyano, T. & Klein, C., 1989. Phase equilibria in the system K_2O-FeO-MgO-Al_2O_3-SiO_2-H_2O-CO_2 and the stability limit of stilpnomelane in metamorphosed Precambrian iron-formations. *Contributions to Mineralogy and Petrology*, **102,** 478–491.

O'Hanley, D. S., Schandl, E. S. & Wicks, F. J., 1992. The origin of rodingites from Cassiar, British Columbia, and their use to estimate T and P ($_{H2O}$) during serpentinization. *Geochimica et Cosmochimica Acta*, **56,** 97–108.

Okay, A. I., 1980. Mineralogy, Petrology and Phase Relations of Glaucophane-Lawsonite Zone Blueschists from the Tavsanli Region, Northwest Turkey. *Contributions to Mineralogy and Petrology*, **72,** 243–255.

Peacock, S. M., 1993. The importance of blueschist => eclogite dehydration reactions in subducting oceanic crust. *Geological Society of America Bulletin of the*, **105,** 684–694.

Powell, R. & Holland, T. J. B., 1988. An internally consistent thermodynamic dataset with uncertainties and correlations: 3. Application methods, worked examples and a computer program. *Journal of Metamorphic Geology*, **6,** 173–204.

Puchkov, V. N., 1997. Structure and geodynamics of the Uralian orogen. In: *Orogeny Through Time, Geological Society Special Publications 121*, (eds Burg, J. P. & Ford, M.) pp. 201–236, Geological Society, London.

Rice, J. M., 1983. Metamorphism of rodingites: Part I. Phase relations in a portion of the system CaO-MgO-Al_2O_3-SiO_2-CO_2-H_2O. *American Journal of Science*, **238,** 121–150.

Rösli, U., Hoernes, S. & Köppel, V., 1991. Isotope data of metarodingites and associated rocks from the Lanzo and the Bracco ophiolitic massifs: Indications on the evolution of the Alpine-type ultramafic-mafic complexes. *Schweizerische Mineralogische und Petrographische Mitteilungen*, **71,** 125–141.

Schandl, E. S., O'Hanley, D. S. & Wicks, F. J., 1989. Rodingites in the serpentinized ultramafic rocks of the Abitibi Greenstone Belt, Ontario. *Canadian Mineralogist*, **27,** 579–591.

Schulte, B. A. & Blümel, P., 1999. Metamorphic evolution of eclogite and associated garnet-mica schist in the high-pressure metamorphic Maksyutov Complex, Ural, Russia. *Geologische Rundschau*, **87,** 561–577.

Shatsky, V. S., Jagoutz, E. & Koz'Menko, O. A., 1997. Sm-Nd dating of the high-pressure metamorphism of the Maksyutov complex, Southern Urals. *Transactions Russian Academy of Science (Translated from Doklady Akademii Nauk)*, **353,** 285–288.

Sobolev, N. V., Dobretsov, N. L., Bakirov, A. B. & Shatsky, V. S., 1986. Eclogites from various types of metamorphic complexes in the USSR and the problems of their origins. In: *Blueschists and Eclogites Memoirs of the Geological Society, 164*, (eds Evans, B. W. & Brown, E. H.), pp. 349–364, Geological Society of America, Boulder.

Staudigel, H., Hart, S. R. & Richardson, S. H., 1981. Alteration of the Oceanic Crust: Processes and timing. *Earth and Planetary Science Letters*, **52,** 311–327.

Thayer, T. P., 1966. Serpentinization Considered as a Constant-Volume Metasomatic Process. *American Mineralogist*, **51,** 685–710.

Tracy, R. J., 1982. Compositional zoning and inclusions in metamorphic minerals. In: *Characterization of Metamorphism Through Mineral Equilibria* (ed. Ferry, J. M.), pp. 355–397. Mineralogical Society America, Washington DC.

Trouw, R. A. J., Simoes, L. S. A. & Valladares, C. S., 1998. Metamorphic evolution of a subduction complex, South Shetland Islands, Antarctica. *Journal of Metamorphic Geology*, **16,** 475–490.

Valizer, P. M. & Lennykh, V. I., 1988. *Amphiboles of Blueschists of the Urals*. Nauka press, Moscov (in Russian).

Zakharov, O. A. & Puchkov, V. N., 1994. On the tectonic nature of the Maksyutovo complex of the Ural-Tau zone. Ufimian. Science Centre, Russian Academy of Science, Ufa (in Russian).

Received 15 November 2000; revision accepted 13 January 2002.

APPENDIX

Mineral compositions were analysed by wavelength dispersive X-ray analyses with an CAMECA SX 50 electron microprobe at the Institute of Chemical Analytics with automated PAP correction at the Technical University Darmstadt. Rb–Sr isotope compositions were analysed with a FINNIGAN MAT 261 solid source mass spectrometer at the Institute of Geowissenschaften und Lithosphärenforschung, University Gießen and the bulk rock composition was analysed by X-ray fluorescence at the Institute of Mineralogy, University of Würzburg.

For the separation of mineral fractions the samples have been crushed to pieces of the minimum diameter of the pseudomorphs. This fraction has been used for handpicking of pseudomorph parts free of matrix material which were then ground again to smaller fractions and separated conventionally to pure mineral fractions. Bulk samples and mineral fractions were dissolved in a HF-HNO_3 mixture and Rb and Sr were separated by cation exchange techniques using SrSpec of EichromIndustries and according Birck & Allègre (1978). Rb–Sr isotopic ratio measurements were made on a multi-collector Finnigan MAT 261 solid source mass spectrometer. Repeated analyses ($n = 23$) of the $^{87}Sr/^{86}Sr$ ratio of the NBS 987 Sr standard during the period of analytical activity yielded 0.71023 ± 0.00003 (2σ of all analyses).

Table A1. Technical data and standards used for automatic WDX analyses.

	Qualitative analyses	Quantitative analyses
High voltage	15 kv	15 kv
Beam current	10–40 nA	10–20 nA
Beam size	1–5 µ	2–7 µ
Resolution	256 × 256 or 512 × 512 pixel	
Measuring time (peak)	200–400 µ s	10–30 s
Background	+ – peak/2	
Crystals	LIF, TAP, PET	LIF, TAP, PET
Standards:		
Anorthite	$CaAl_2Si_2O_8$,Si kα on PET	
Albite	$NaAlSi_3O_8$, Na kα on TAP	
Chromite	Cr_2O_3, Cr kα on LIF	
corundum	Al_2O_3, Al kα on TAP	
diopside	$CaMgSi_2O_6$, Mg kα on TAP	
hematite	Fe_2O_3, Fe kα on LIF	
orthoclase	$KAlSi_3O_8$, K kα on PET	
rhodonite	$MnSiO_3$, Mn kα on LIF	
rutile	TiO_2, Ti kα on LIF	
wollastonite	$CaSiO_3$, Ca kα on PET	

Repeated analyses of the standards ($n = 5$–12) results in $< 0.1\%$ between 100 and 5 wt% oxide, $> 2\%$ between 5 and 2 wt% oxide and $> 30\%$ $< 2\%$ wt% oxides (2σ of all analyses).